https://doi.org/10.1093/plphys/kiac026 PLANT PHYSIOLOGY 2022: 188: 2073–2084

Plant Physiology®

Research Article

Autophagy is required for self-incompatible pollen rejection in two transgenic *Arabidopsis thaliana* accessions

Stuart R. Macgregor,[1] Hyun Kyung Lee ,[1,†] Hayley Nelles,[1] Daniel C. Johnson ,[1] Tong Zhang,[2] Chaozhi Ma[2] and Daphne R. Goring [1,3,*,‡]

1 Department of Cell & Systems Biology, University of Toronto, Toronto, Canada M5S 3B2
2 National Key Laboratory of Crop Genetic Improvement, National Center of Rapeseed Improvement in Wuhan, Huazhong Agricultural University, Wuhan 430070, China
3 Centre for the Analysis of Genome Evolution & Function, University of Toronto, Toronto, Canada M5S 3B2

*Author for correspondence: d.goring@utoronto.ca
†Present address: Department of Plant Molecular Biology, University of Lausanne, Lausanne, Switzerland.
‡Senior author

D.R.G. conceived the project. D.R.G., S.R.M., H.K.L., H.N., D.C.J., and T.Z. conceptualized and designed the experiments; S.R.M. performed crosses, generated and analyzed data for the SI-C24 atg7-9 plants, SI-Col-0 atg5-1 plants, and the SI-Col-0 atg7-2 GFP-ATG8a imaging. H.K.L. and S.R.M. performed crosses, generated and analyzed data for the SI-Col-0 atg7-2 plants. H.N. and D.C.J. performed preliminary work on the SI lines and imaging; T.Z. generated the SI-Col-0 line. D.R.G. and C.M. supervised the experiments. S.R.M., H.K.L., and D.R.G. wrote the manuscript. All authors commented on the manuscript before submission. D.R.G. agrees to serve as the author responsible for contact and ensures communication.
The author responsible for distribution of materials integral to the findings presented in this article in accordance with the policy described in the Instructions for Authors (https://academic.oup.com/plphys/pages/general-instructions) is Daphne Goring (d.goring@utoronto.ca).

Abstract

Successful reproduction in the Brassicaceae is mediated by a complex series of interactions between the pollen and the pistil, and some species have an additional layer of regulation with the self-incompatibility trait. While the initial activation of the self-incompatibility pathway by the pollen *S*-locus protein 11/*S* locus cysteine-rich protein and the stigma *S* Receptor Kinase is well characterized, the downstream mechanisms causing self-pollen rejection are still not fully understood. In previous studies, we detected the presence of autophagic bodies with self-incompatible (SI) pollinations in *Arabidopsis lyrata* and transgenic *Arabidopsis thaliana* lines, but whether autophagy was essential for self-pollen rejection was unknown. Here, we investigated the requirement of autophagy in this response by crossing mutations in the essential *AUTOPHAGY7* (*ATG7*) and *ATG5* genes into two different transgenic SI *A. thaliana* lines in the Col-0 and C24 accessions. By using these previously characterized transgenic lines that express *A. lyrata* and *Arabidopsis halleri* self-incompatibility genes, we demonstrated that disrupting autophagy weakened their SI responses in the stigma. When the *atg7* or *atg5* mutations were present, an increased number of SI pollen was found to hydrate and form pollen tubes that successfully fertilized the SI pistils. Additionally, we confirmed the presence of GFP-ATG8a-labeled autophagosomes in the stigmatic papillae following SI pollinations. Together, these findings support the requirement of autophagy in the self-incompatibility response and add to the growing understanding of the intracellular mechanisms employed in the transgenic *A. thaliana* stigmas to reject self-pollen.

Received October 07, 2021. Accepted December 22, 2021. Advance access publication January 25, 2022

Introduction

Reproduction in the Brassicaceae is a tightly controlled process, with many components contributing to successful pollen–pistil interactions (reviewed in Mizuta and Higashiyama, 2018; Johnson et al., 2019; Adhikari et al., 2020; Abhinandan et al., 2021). The Brassicaceae dry stigma lacks surface secretions and instead regulates the delivery of resources to the pollen shortly after pollination. This leads to the selective hydration of compatible pollen grains, followed by the penetration of the pollen tube into the stigmatic barrier to grow down the reproductive tract (reviewed in Dickinson, 1995; Palanivelu and Tsukamoto, 2012; Adhikari et al., 2020; Abhinandan et al., 2021). It is also at this initial cell–cell communication stage that self-incompatible (SI) pollen is recognized and blocked by the stigma to prevent inbreeding (reviewed in Nasrallah, 2019; Durand et al., 2020; Abhinandan et al., 2021). A recent live-cell imaging study in *Arabidopsis thaliana* compared pollen hydration rates of compatible and SI pollen grains and found that while compatible pollen grains rapidly hydrated, SI pollen failed to fully hydrate which then led to a failure in pollen germination or a failure of pollen tubes to penetrate the stigmatic papilla cell wall (Rozier et al., 2020). Furthermore, actin foci were present in the stigmatic papillae at the site of emerging pollen tubes for compatible pollen only. The actin focalization is likely associated with the stigmatic papilla cellular responses to enable compatible pollen hydration and pollen tube penetration (Rozier et al., 2020).

The Brassicaceae SI response is initiated by the binding of the S-haplotype-specific pollen ligand, S-locus protein 11/S locus cysteine-rich protein (SP11/SCR) to the corresponding stigma-specific S Receptor Kinase (SRK). This leads to the phosphorylation of the SRK kinase domain and activation of the downstream signaling responses, ultimately leading to the rejection of the SI pollen grain (reviewed in Nasrallah, 2019; Abhinandan et al., 2021). Not all Brassicaceae species possess this trait due to mutations in the key self-incompatibility genes, *SP11/SCR* and *SRK* (reviewed in Durand et al., 2020). For example, the transition of *A. thaliana* to a fully selfing species is associated with mutations in the *SCR* and *SRK* genes (Kusaba et al., 2001; Shimizu et al., 2008; Boggs et al., 2009; Tsuchimatsu et al., 2010; Guo et al., 2011; Tsuchimatsu et al., 2017). In contrast, other family members like *Arabidopsis lyrata* and *Arabidopsis halleri* have intact *SCR* and *SRK* genes, which result in a robust self-incompatibility response upon self-pollination (Kusaba et al., 2001; Schierup et al., 2001; Goubet et al., 2012).

A number of studies have reintroduced the self-incompatibility trait back into *A. thaliana* by introducing *A. lyrata* or *A. halleri SP11/SCR* and *SRK* transgenes (Nasrallah et al., 2004; Boggs et al., 2009; Indriolo et al., 2014a, 2014b; Iwano et al., 2015; Zhang et al., 2019; Rozier et al., 2020). However, the success of this approach was accession-dependent; for example, transgenic experiments in *A. thaliana* Col-0 failed to produce SI plants, whereas experiments using *A. thaliana* C24 were very successful (Nasrallah et al., 2004; Boggs et al., 2009; Iwano et al., 2015). The cause of this was linked to inverted repeats within the *A. thaliana SRKA* pseudogene which triggers RNA silencing of the introduced *SRK* transgenes (Fujii et al., 2020). For the Col-0 accession, the inverted repeat was found in a conserved region of the predicted *pseudoSRKA* kinase domain resulting in the silencing of closely related *SRK* transgenes. For the C24 accession, the inverted repeat was found in a more polymorphic region of the predicted *pseudoSRKA* ectodomain and appeared to be less effective at inducing RNA silencing of related *SRK* transgenes (Fujii et al., 2020).

We have found that a strong SI response can also be recapitulated in *A. thaliana* Col-0 when the *A. lyrata* or *A. halleri ARM Repeat Containing 1* (*ARC1*) transgene was added along with the *A. lyrata* or *A. halleri SP11/SCR* and *SRK* transgenes (Indriolo et al., 2014a, 2014b; Zhang et al., 2019). The ARC1 E3 ubiquitin ligase is proposed to act directly downstream of SRK in the self-incompatibility signaling pathway (Gu et al., 1998; Stone et al., 1999, 2003); reviewed in Abhinandan et al. (2021). A large part of the *ARC1* gene has been deleted in the *A. thaliana* genome, and knockdowns of *ARC1* in SI *Brassica napus* and *A. lyrata* resulted in a partial breakdown of self-incompatibility (Stone et al., 1999; Indriolo et al., 2012). ARC1 is proposed to target cellular components that are required in the stigma to accept compatible pollen, such as the EXO70A1 exocyst subunit (Samuel et al., 2009) and *Brassica* Glyoxalase I (GLO1) and Phospholipase D (Sankaranarayanan et al., 2015; Scandola and Samuel, 2019). SI pollinations in transgenic *A. thaliana* SI-C24 plants also induced a strong and rapid cytosolic calcium influx in the stigmatic papillae (Iwano et al., 2015). These combined self-incompatibility responses are proposed to disrupt the secretory activity in the stigmatic papillae which would be required for compatible pollen acceptance (Elleman and Dickinson, 1996; Samuel et al., 2009; Safavian and Goring, 2013; Safavian et al., 2015); reviewed in Dickinson (1995), Goring (2017), and Abhinandan et al. (2021).

In previous work, we uncovered signs of autophagy activation in SI *A. lyrata* and transgenic *A. thaliana* SI-Col-0 stigmatic papillae within 10 min of SI pollinations, but not with compatible pollinations (Safavian and Goring, 2013; Indriolo et al., 2014a, 2014b). Transmission electron microscopy (TEM) images revealed structures resembling autophagic bodies in the vacuoles of stigmatic papilla following SI pollinations (Safavian and Goring, 2013; Indriolo et al., 2014a, 2014b). In contrast, TEM images of compatible pollinations revealed vesicle-like structures in the stigmatic papillae under the compatible pollen contact site suggestive of secretory activity (Safavian and Goring, 2013; Indriolo et al., 2014a, 2014b). The presence of autophagosomes in *A. lyrata* SI pollinations was further confirmed using the GFP-ATG8a autophagosome marker (Safavian and Goring, 2013). Although these studies indicated that autophagy was activated following SI pollinations, it was unclear whether autophagy is

essential for the rejection of SI pollen. Here, we have used two different transgenic *A. thaliana* SI lines (in the Col-0 and C24 accessions; Iwano et al., 2015; Zhang et al., 2019) to test the requirement of the autophagy system for self-pollen rejection. When loss-of-function mutants in the *AUTOPHAGY7* (*ATG7*) and *ATG5* genes (Chung et al., 2010; Ding et al., 2018) were combined with the SI-Col-0 and SI-C24 lines, we observed a partial breakdown of the self-incompatibility response in both accessions. This indicates that autophagy is an additional intracellular mechanism by which SI pollen is effectively rejected in both transgenic *A. thaliana* SI lines.

Results

Generation of SI *A. thaliana* transgenic lines carrying the *atg7* and *atg5* mutations to disrupt autophagy

To investigate the involvement of autophagy in self-incompatibility, two different transgenic *A. thaliana* SI lines were used to cross with *atg7* and *atg5* autophagy mutants. ATG7 and ATG5 are essential components in the formation of autophagosomes (reviewed in (Ding et al., 2018), and both the *atg7* and *atg5* mutations lead to a loss of autophagy (Thompson et al., 2005; Chung et al., 2010; Young et al., 2019). The first SI line is in the Col-0 accession (SI-Col-0) and carries the *A. halleri SCR13*, *SRK13*, and *ARC1* transgenes in a single T-DNA (*Ah-SCR13 Ah-SRK13 Ah-ARC1* #2 line; Zhang et al., 2019). This SI-Col-0 line was crossed to the previously characterized *atg7-2* mutant in the Col-0 accession (Chung et al., 2010). The F_1 plants from this cross were selfed, and all pollination assays were carried out in the F_2 generation. To confirm that any observed effects were not specific to the loss of *ATG7*, the previously characterized *atg5-1* mutation in the Col-0 accession (Thompson et al., 2005) was also crossed into the SI-Col-0 line, and taken to the F_2 generation for pollination assays. The second SI line is in the C24 accession (SI-C24) and carries the *A. lyrata SCRb* and *SRKb* transgenes (SI-C24 #15-1 line; Iwano et al., 2015). As there were no *atg7* mutants available in the C24 accession, CRISPR/Cas9 technology was used to generate additional *atg7* mutants. Deletion of the *ATG7* gene was confirmed through PCR and sequencing of genomic regions flanking gRNA target sites (Supplemental Figure S1). The *atg7-9* C24 mutant displayed the same overall wild-type plant and flower morphology (Supplemental Figure S2) as seen for the *atg7-2* Col-0 mutant. The C24 *atg7-9* mutant was crossed with the SI-C24 line, and following selfing of the F_1 plants, all pollination assays were carried out in F_2 generation (T_4 generation for the *atg7-9* mutation). For all three sets of F_2 progeny, genotyping was first carried out to identify the transgenic plants carrying the SI transgenes, followed by genotyping for the *atg7* or atg5 mutations to identify plants that were wild-type or homozygous for the *atg* mutations.

Disrupting autophagy breaks down the initial SI response of blocking pollen hydration

To assess the early stages of pollen rejection, the pollen hydration checkpoint was first investigated. SI pollen from the parental SI-Col-0 or SI-C24 transgenic lines were used to pollinate pistils from the respective F_2 progeny segregating for the *atg7* or *atg5* mutations, and pollen hydration assays were carried out by measuring the increase in pollen diameter at 10-min postpollination (Lee et al., 2020). Positive controls of the SI-Col-0 and SI-C24 pollen placed on compatible wild-type Col-0 and C24 pistils, respectively, resulted in a large increase in diameter as a result of pollen hydration (Figure 1, A and B). In contrast, self-pollen placed on the SI-

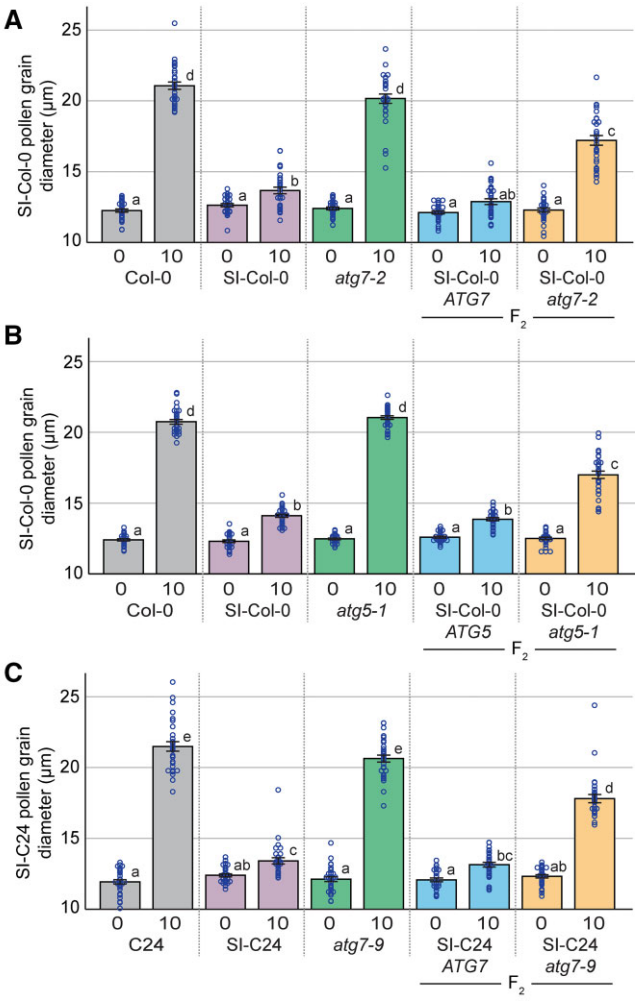

Figure 1 Pollen hydration assays on control and SI F_2 progeny segregating for the *atg7* and *atg5* mutations. Pollen hydration assays for (A), SI-Col-0 pollen grains placed on stigmas from Col-0, SI-Col-0, *atg7-2*, and F_2 progeny from the SI-Col-0 x *atg7-2* cross; (B) SI-Col-0 pollen grains placed on stigmas from Col-0, SI-Col-0, *atg5-1*, and F_2 progeny from the SI-Col-0 x *atg5-1* cross; and (C) SI-C24 pollen grains placed on stigmas from C24, SI-C24, *atg7-9*, and F_2 progeny stigmas from the SI-C24 × *atg7-9* cross. Pollen hydration was measured by taking pollen grain diameters at 0- and 10-min postpollination. Data are shown as mean ± SE with all data points displayed. $n = 30$ pollen grains per line, $P < 0.05$ (one-way ANOVA with Tukey's HSD post-hoc test).

Col-0 and SI-C24 pistils resulted in very little pollen hydration at 10-min postpollination (Figure 1, A and B). This lack of hydration was consistent between the SI-Col-0 and SI-C24 lines and indicative of the early recognition and rejection of SI pollen. Importantly, stigmas from the *atg7-2*, *atg5-1*, *and atg7-9* mutants showed normal SI-Col-0 and SI-C24 pollen hydration, respectively, indicating that disruption in the autophagic process did not perturb the compatible postpollination responses (Figure 1, A and B).

For the F_2 progeny from the SI-Col-0 x *atg7-2* cross, the SI-Col-0 plants homozygous for wild-type *ATG7* showed the same small increase in pollen hydration as the control SI pollinations at 10-min postpollination. In contrast, when SI-Col-0 pollen was applied to the SI-Col-0 stigmas that were homozygous for the *atg7-2* mutation, an increase in pollen hydration was observed, indicating an incomplete rejection of the SI pollen (Figure 1A). Similarly, pollen hydration assays on the F_2 progeny from the SI-Col-0 × *atg5-1* cross showed that hydration of SI-Col-0 pollen on SI-Col-0 stigmas wild-type for *ATG5* displayed a small increase while SI-Col-0 pollen hydration on SI-Col-0 stigmas homozygous for the *atg5-1* mutation was significantly increased (Figure 1B). A comparable set of pollen hydration experiments on the F_2 progeny from the SI-C24 × *atg7-9* cross also showed a similar trend (Figure 1C). SI-C24 stigmas that were wild-type for *ATG7* supported similar small increases in SI-C24 pollen hydration as the control SI pollinations, and the introduction of the *atg7-9* mutation into this background resulted in increased hydration of the SI pollen. Together, these results indicate that autophagy is required to fully prevent the hydration of SI pollen.

Disruption of autophagy increases SI pollen tube penetration

With the observed increase in SI pollen hydration, the next stage of preventing SI pollen germination and pollen tube

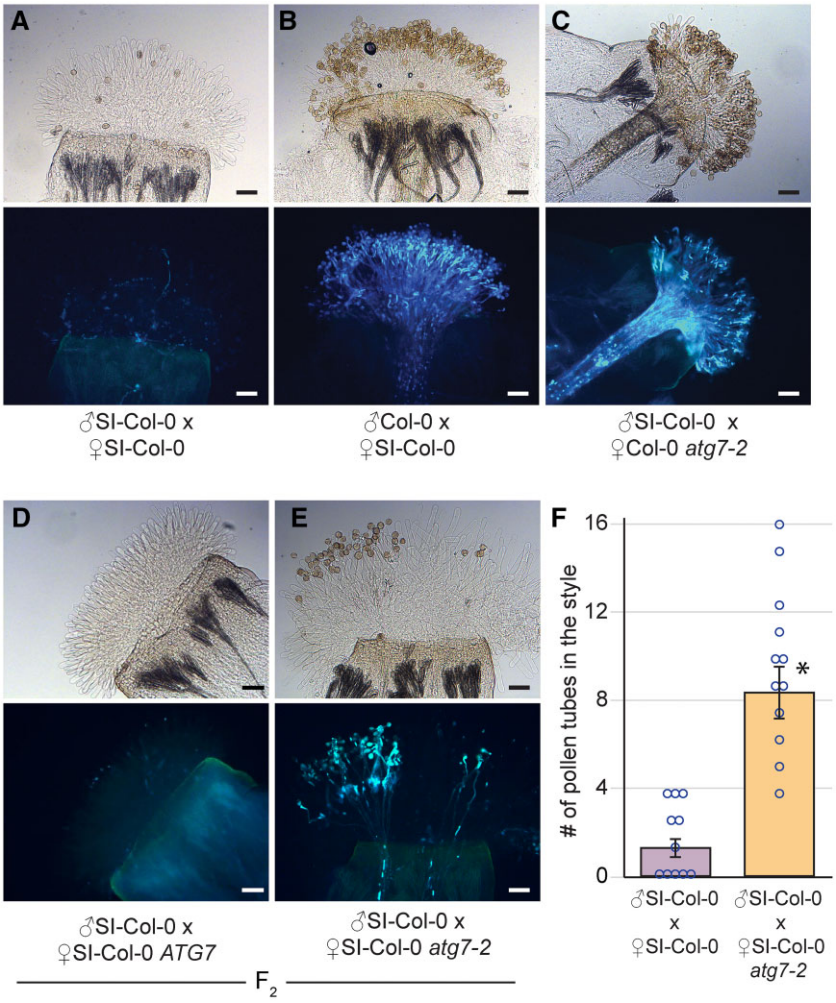

Figure 2 Representative images of aniline blue-stained SI-Col-0 or SI-Col-0 *atg7-2* pistils at 24 h following pollination. A–E, All stigmas were hand-pollinated with SI-Col-0 pollen or wild-type Col-0 pollen as indicated and collected at 24-h postpollination for aniline blue staining. The genotypes of the pistils are indicated for each panel. Pollen tubes penetrating through the stigma and style indicate a breakdown of self-incompatibility as seen in (E). For each panel, top image = brightfield, bottom image = aniline blue. Scale bar = 100 µm. F, Bar graph showing the mean number of pollen tubes at 24-h postpollination. Data are shown as mean ± SE with all data points displayed. n = 11–12 pistils per line. At 24-h, pistils from SI-Col-0 *atg7-2* mutants allowed a significantly higher number of SI-Col-0 pollen tubes compared to the SI-Col-0 pistils. ($P < 0.05$, Student's t test).

penetration was investigated. To determine if this block was affected by the *atg7* and *atg5* mutations, pollinated pistils were collected at 2- and 24-h postpollination and stained with aniline blue to visualize pollen tubes. At 2-h postpollination, SI-Col-0 and SI-C24 pollen was completely rejected by the respective SI pistils, and no pollen tubes were visible (Supplemental Figures S3 and S4). Although we did not see any obvious difference at 2-h postpollination, we did observe an occasional pollen tube that penetrated the stigma barrier of the SI-Col-0 and SI-C24 *atg* homozygous mutants. To address whether we could observe a greater number of SI-Col-0 and SI-C24 pollen tubes after a longer period, pollinated pistil samples were then harvested at 24-h postpollination. A later time point following pollination is more reflective of the natural pollination process and provides more time for the SI pollen to germinate and grow into the pistil. Self-pollination of the SI-Col-0 and SI-C24 parental lines resulted in an absence of pollen tubes (Figures 2, A, 3, A, and 4, A), while pollinations with compatible wild-type pollen led to an abundance of pollen tubes growing in the pistils (Figures 2, B, 3, B, and 4, B). The results indicated that the SI-Col-0 and SI-C24 pistils were able to fully reject SI pollen and accept wild-type compatible pollen at 24-h postpollination. The SI-Col-0 and SI-C24 pollen also produced numerous pollen tubes when placed on the *atg* mutant pistils, indicating that the absence of autophagy did not affect these compatible pollinations (Figures 2, C and 3, C). The impact of the *atg* mutations on self-incompatibility at 24-h postpollination was examined by applying the SI-Col-0 and SI-C24 pollen on their respective F_2 progeny homozygous for the *atg* mutations. When SI-Col-0 *atg7-2* stigmas or SI-Col-0 *atg5-1* stigmas were pollinated with SI-Col-0 pollen, there was a general increase in the number of pollen grains adhering to the stigma and forming pollen tubes when compared to the SI-Col-0 pistils (Figures 2, D–F and 3, D–F). The pollinations were repeated for the SI-C24 F_2 plants, and

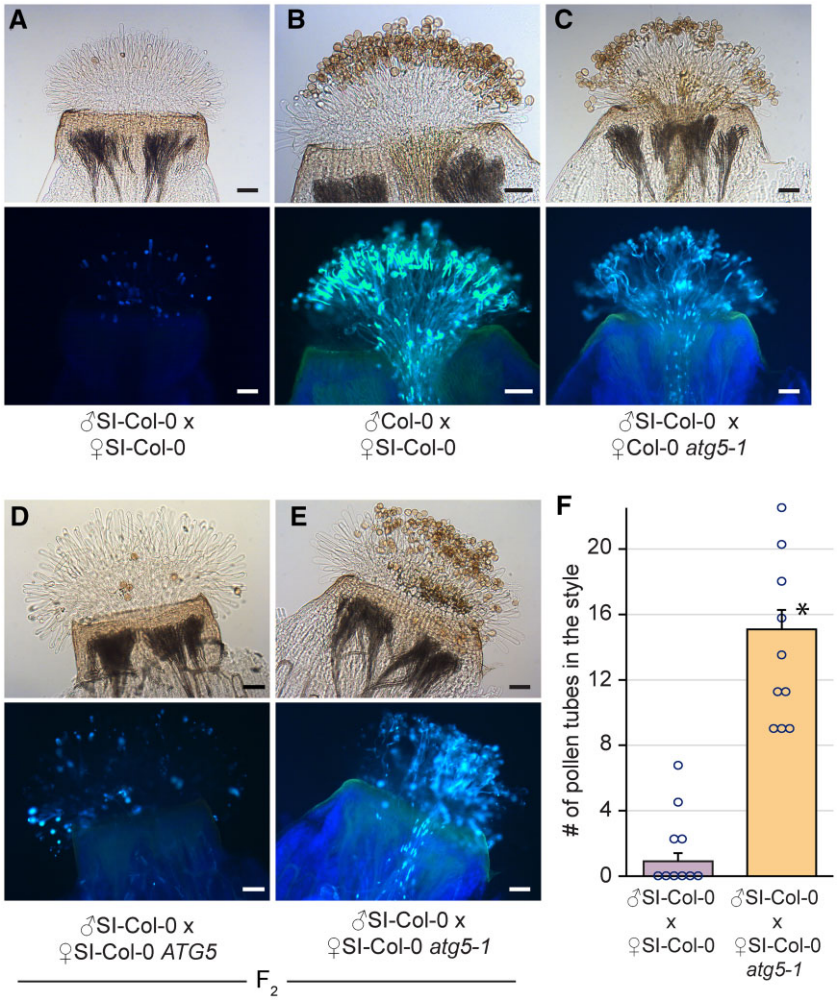

Figure 3 Representative images of aniline blue-stained SI-Col-0 or SI-Col-0 *atg5-1* pistils at 24 h following pollination. A–E, All stigmas were hand-pollinated with SI-Col-0 pollen or wild-type Col-0 pollen as indicated and collected at 24-h postpollination for aniline blue staining. The genotypes of the pistils are indicated for each panel. Pollen tubes penetrating through the stigma and style indicate a breakdown of self-incompatibility as seen in (E). For each panel, top image = brightfield, bottom image = aniline blue. Scale bar = 100 μm F, Bar graph showing the mean number of pollen tubes at 24 h postpollination. Data are shown as mean ± SE with all data points displayed. n = 10 pistils per line. At 24 h, pistils from SI-Col-0 *atg5-1* mutants allowed a significantly higher number of SI-Col-0 pollen tubes compared to the SI-Col-0 pistils ($P < 0.05$, Student's t test).

again the SI-C24 *atg7-9* pistils did show some SI-C24 pollen adhering to the stigmatic surface and successfully growing pollen tubes through the pistil while the SI-C24 *ATG7* pistils rejected the SI-C24 pollen (Figure 4, D–F). The number of pollen tubes was counted in the SI-Col-0 and SI-C24 pistils that were wild-type or homozygous for the *atg* mutations, and a significant increase in the number of pollen tubes were counted in the homozygous *atg7* and *atg5* mutants (Figures 2, F, 3, F, and 4, F). Thus, the 24-h postpollination samples demonstrated that autophagy is required for fully blocking SI pollen germination and pollen tube growth through the SI pistil.

Loss of autophagy increases seed set in the SI lines

With the observation that self-incompatibility is partially lost in the SI-Col-0 *atg7-2*, SI-Col-0 *atg5-1*, and SI-C24 *atg7-9* mutant pistils, resulting in more pollen tubes growing through the pistils, the impact of this on seed set was assessed. Manual pollinations were carried out using SI-Col-0 and SI-C24 pollen on pistils from the respective parental lines and F_2 progeny homozygous for the *atg7* or *atg5* mutations, and 2-week-old siliques were harvested for seed counting (Figure 5; Supplemental Figure S5). As expected for compatible pollinations in Col-0, C24, and the *atg* mutants, abundant seeds/silique were produced (Figure 5, A–C). As well, self-pollinations of SI-Col-0 and SI-C24 pistils resulted in a very limited seed yield consistent with the rejection of SI pollen (Figure 5, A–C). When the SI-Col-0 *atg7-2* pistils were pollinated with SI-Col-0 pollen, there was a significant increase in yield to 27 seeds/silique compared to 12.8 seeds/silique for SI-Col-0 indicating an incomplete rejection of the SI-Col-0 pollen by the SI-Col-0 *atg7-2* pistils (Figure 5A). Similarly, when SI-Col-0 *atg5-1* pistils were pollinated with SI-Col-0 pollen, there was an increased average yield of 31.9

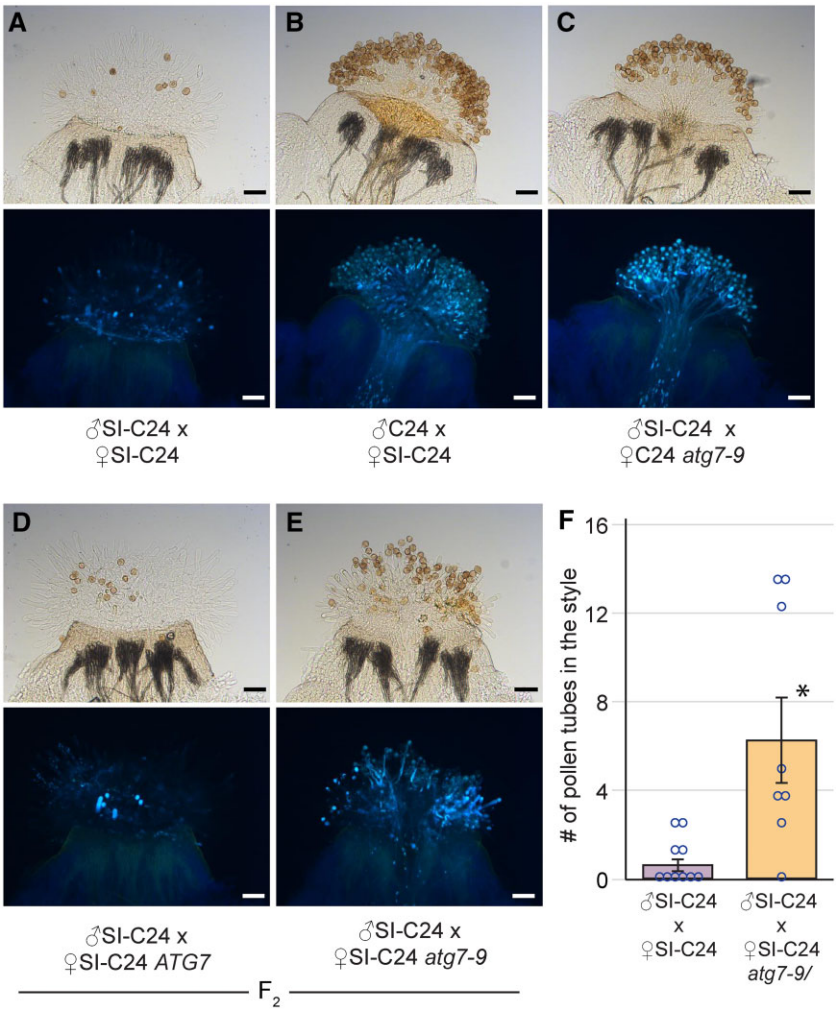

Figure 4 Representative images of aniline blue-stained SI-C24 or SI-C24 *atg7-9* pistils at 24 h following pollination. A–E, All stigmas were hand-pollinated with SI-C24 pollen or wild-type C24 pollen as indicated and collected at 24-h postpollination for aniline blue staining. The genotypes of the pistils are indicated for each panel. Pollen tubes penetrating through the stigma and style indicate a breakdown of self-incompatibility as seen in (E). For each part, top image = brightfield, bottom image = aniline blue. Scale bar = 100 μm. F, Bar graph showing the mean number of pollen tubes at 24-h postpollination. Data are shown as mean ± SE with all data points displayed. n = 8–10 pistils per line. At 24-h, pistils from SI-C24 *atg7-9* mutants allowed a significantly higher number of SI-C24 pollen tubes compared to the SI-C24 pistils ($P < 0.05$, Student's t test).

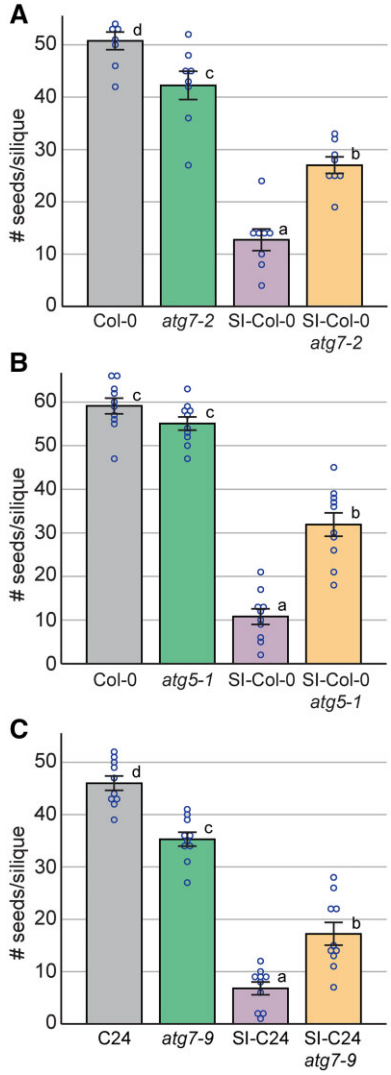

Figure 5 Seeds per silique counts for control and SI F_2 progeny with the *atg7* or *atg5* mutations. Seeds per silique counts following manual pollination with (A), (B), SI-Col-0 pollen or (C), SI-C24 pollen on pistils with the indicated genotypes. Siliques were harvested at 2-week post-pollination and cleared for seeds counts. Data are shown as mean ± SE with all data points displayed. n = 8–10 siliques per line. Compared to the control SI pollinations, significant increases in the number of seeds per silique were observed for the SI plants that were homozygous for the *atg7* or *atg5* mutations, $P < 0.05$ (one-way ANOVA with Tukey's HSD post-hoc test).

seeds/silique compared to 10.8 seeds/silique for SI-Col-0 (Figure 4B). Finally, similar trends in seed yields were observed in the C24 accession. SI pollinations with SI-C24 pistils resulted in a low average of 6.8 seeds/silique as expected yet when the SI-C24 *atg7-9* pistils were pollinated with SI-C24 pollen, there was a significant increase in seed yields to 17.2 seeds/silique (Figure 5C). Altogether, these results indicate that loss of autophagy was sufficient to disrupt the self-incompatibility pathway allowing for the growth of more SI pollen tubes through the SI-Col-0 and SI-C24 pistils carrying *atg7* or *atg5* mutations to initiate fertilization and seed production, and thus, confirming that autophagy is required for full rejection of self-pollen.

Autophagosomes are produced following self-pollination in the SI-C24 line

Previously, autophagosomes were detected by TEM following SI pollinations in *A. lyrata* and in the transgenic *A. thaliana* SI-Col-0 transformed with *A. lyrata* S-locus genes (Safavian and Goring, 2013; Indriolo et al., 2014a, 2014b). To confirm that autophagosomes are also forming in the SI-Col-0 *Ah-SCR13 Ah-SRK13 Ah-ARC1* #2 line used in this study, *GFP-ATG8a* was used as an autophagosome marker (Thompson et al., 2005). Col-0 plants carrying the *ProUBQ10:GFP-ATG8a* construct (Kim et al., 2013) were crossed with the SI-Col-0 line, and the subsequent F_1 generation was used for imaging. The SI-Col-0 *GFP-ATG8a* stigmas were imaged as unpollinated or manually pollinated with either Col-0 or SI-Col-0 pollen. At 15-min postpollination, many GFP punctae were observed in the SI-Col-0 *GFP-ATG8a* stigmatic papillae contacting SI-Col-0 pollen (Figure 6A). Conversely, few puncta were observed in either unpollinated SI-Col-0 GFP-ATG8a stigmatic papillae or those pollinated with Col-0 pollen, consistent with a low background level of autophagy (Figure 6, C and E). The number of puncta were counted for both SI-Col-0 pollinated, Col-0 pollinated and unpollinated SI-Col-0 GFP-ATG8a stigmatic papillae (Figure 6G), and there was a significant increase in the number of GFP-ATG8a-labeled punctae in the SI-pollinated SI-Col-0 *GFP-ATG8a* stigmatic papillae indicating a strong induction of autophagy. These observations confirm our previous findings that autophagy is activated in the stigmatic papillae with SI pollinations when compared to a compatible pollinated or unpollinated stigma (Safavian and Goring, 2013; Indriolo and Goring, 2014).

Discussion

Self-incompatibility plays an important regulatory role in many outcrossing Brassicaceae species where producing inbred progeny would be disadvantageous (Shimizu and Tsuchimatsu, 2015; Durand et al., 2020). Previous studies have uncovered many important steps in the self-incompatibility pathway, but there are still outstanding questions on the cellular mechanisms by which self-pollen is rejected (reviewed in Goring, 2017; Jany et al., 2019; Abhinandan et al., 2021). In previous studies, we observed the presence of autophagosomes in the cytoplasm and autophagic bodies in the vacuole following SI pollinations in SI *A. lyrata* and transgenic *A. thaliana* SI-Col-0 lines (Safavian and Goring, 2013; Indriolo and Goring, 2014). What was not known, however, was whether autophagy was necessary for SI pollen rejection. In this study, we addressed this question by crossing two different autophagy-deficient mutants (*atg7* and *atg5*) into two different transgenic *A. thaliana* SI-lines and demonstrated that a functioning autophagy system is required in the stigma for the full rejection of SI pollen. It is important to note that

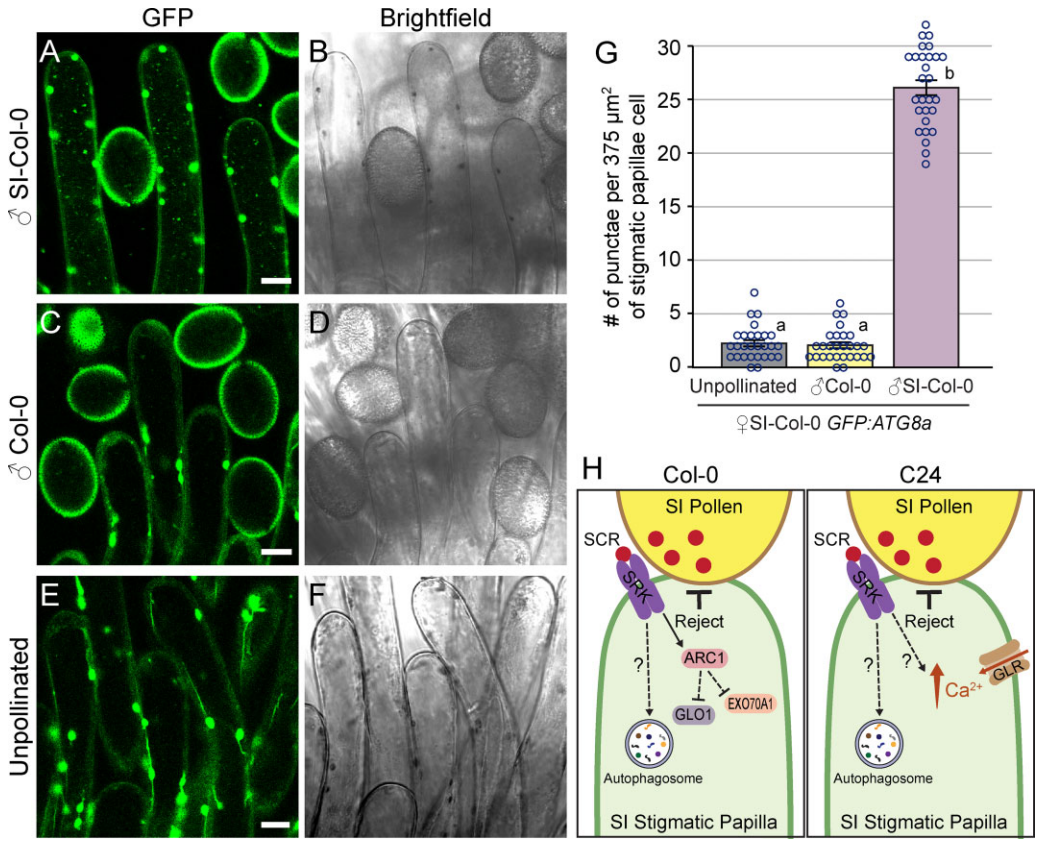

Figure 6 Autophagosomes are more abundant in SI-Col-0 *GFP-ATG8a* papillae following pollination with SI-Col-0 pollen. A–F, Representative images showing that more GFP-ATG8a-labeled autophagosomes marked by GFP-ATG8a are visible at 15-min postpollination in the SI-Col-0 *GFP-ATG8a* papillae pollinated with SI-Col-0 pollen (A and B) compared to Col-0 pollinated (C and D) or unpollinated (E and F) SI-Col-0 *GFP-ATG8a* papillae. Scale bar = 10 µm. G, Bar graph showing the mean number of autophagosomes present in each sample. Data are shown as mean ± SE with all data points displayed. n = 28 papillae from six stigmas for each set of data. At 15-min postpollination with SI-Col-0 pollen, there is a significant increase in the number of GFP-labeled punctae in the SI-Col-0 *GFP-ATG8a* papillae ($P < 0.05$) (One-way ANOVA with Tukey's HSD post-hoc test). The large punctae are chloroplasts with autofluorescence and were not counted. H, Models for SI pollen rejection in the transgenic *A. thaliana* accessions. Following the self-incompatibility determinants, SP11/SCR and SRK, the specific intracellular cellular mechanisms by which SI pollen is rejected in transgenic *A. thaliana* SI-Col-0 and SI-C24 lines are still not well-understood. These models summarize the known components for each transgenic accession (Samuel et al., 2009; Indriolo et al., 2014a, 2014b; Iwano et al., 2015; Kenney et al., 2020). Here, we show that autophagy is a shared requirement in the stigmatic papillae for both transgenic SI accessions to fully enable SI pollen rejection.

disrupting autophagy did not cause a full loss of self-incompatibility indicating that other cellular responses are required in conjunction with autophagy for SI pollen rejection. Importantly, this partial breakdown in the stigma was seen for all stages from increased pollen hydration to more pollen tubes growing through the pistil to increase seed yields. Finally, the requirement of autophagy in the rejection of SI pollen was consistent between the three different autophagy-deficient mutants (*atg7-2*, *atg7-9*, and *atg5*) and the two different *A. thaliana* accessions (Col-0 and C24) used in the SI lines indicating that this is a shared mechanism for SI pollen rejection.

The rationale for using both the SI-Col-0 and SI-C24 lines was to determine if there were any accession- or transgene-specific associations with autophagy. The SI-Col-0 carries the *A. halleri SCR13*, *SRK13*, and *ARC1* transgenes (Zhang et al., 2019), while the SI-C24 line carries the *A. lyrata SCRb* and *SRKb* transgenes (Iwano et al., 2015). In addition to two different S-haplotypes from two different Arabidopsis species, the SI-Col-0 line also carries the *A. halleri ARC1* transgene. Overall, our results indicate that autophagy is a shared intracellular response in these two transgenic accessions for SI pollen rejection (see models in Figure 6H). The importance of this discovery is related to how little is really known about the intracellular mechanisms employed by these transgenic *A. thaliana* SI-lines. Much of our current understanding of the self-incompatibility pathway relies on knowledge gained from the compatible pollen response pathway in combination with studies on the *Brassica* self-incompatibility system (reviewed in Abhinandan et al., 2021). Many studies have verified the requirements of *SP11/SCR* and *SRK* transgenes for conferring the self-incompatibility trait in *A. thaliana* (Nasrallah et al., 2004; Boggs et al., 2009; Indriolo et al., 2014a, 2014b; Iwano et al., 2015; Zhang et al., 2019; Rozier et al., 2020), but the intracellular mechanisms by which self-pollen rejection occurs in

these transgenic *A. thaliana* SI-lines are still poorly understood (Figure 6H). A role for a rapid cytosolic calcium influx and *GLUTAMATE RECEPTOR-LIKE* (*GLR*) genes in the stigmatic papillae was identified using the transgenic *A. thaliana* SI-C24 plants, but how they are activated in response to SI-pollen is not known (Iwano et al., 2015). As well, EXO70A1 and GLO1 have been linked to the compatible pollen responses in *A. thaliana* Col-0 and SI-Col-0 plants, respectively (Samuel et al., 2009; Kenney et al., 2020), and could be potentially targeted by ARC1 in the *A. thaliana* SI-Col-0 plants (Figure 6H). The fact that both accessions require an intact autophagy system in the stigma for full SI pollen rejection indicates that autophagy activation does not require ARC1, though the potential involvement of another related PUB E3 ligase cannot be ruled out (Indriolo et al., 2012; Indriolo and Goring, 2016).

The question then arises on how autophagy is activated and the purpose of autophagy activation in self-incompatibility. SI pollen carries the signals to be recognized as both SI pollen and compatible pollen, and it has been hypothesized that self-incompatibility blocks compatible pollen responses in the stigma (Dickinson, 1995). With the working model that secretory activity in the stigma is required for compatible pollen acceptance (reviewed in Dickinson, 1995; Goring, 2017; Abhinandan et al., 2021), several of the self-incompatibility cellular responses such as EX070A1 inhibition (Samuel et al., 2009; Sankaranarayanan et al., 2015), a strong and rapid calcium influx (Iwano et al., 2015), and the absence of actin focalization (Rozier et al., 2020) are consistent with blocking secretion (reviewed in Goring, 2017). Autophagy could also be an additional step to clear any secretory activity that was initially activated. With the already established connection of the exocyst for compatible pollen responses (Samuel et al., 2009; Safavian et al., 2014, 2015; Jamshed et al., 2020) and the targeting of EXO70A1 in *Brassica* self-incompatibility (Samuel et al., 2009), it may be that some of the exocyst subunits are redirected toward autophagy during the self-incompatibility response. For example, EXO70B2 is another exocyst subunit involved in secretion, and phosphorylation during immune responses was found to redirect EXO70B2 to autophagosomes for degradation, and this was proposed to reduce secretion (Brillada et al., 2021). Finally, the exocyst subunit, SEC5, has been linked to Rho of Plants GTPase signaling and autophagosome formation under stress conditions (Lin et al., 2021).

In conclusion, this study now firmly places autophagy as part of the cellular mechanisms leading to SI pollen rejection. Future studies will need to focus on how autophagy is activated in the self-incompatibility pathway and whether there are specific cytoplasmic components targeted for autophagic destruction. Understanding the mechanisms underlying self-incompatibility is important as seed yield of many important crop species is directly tied to their reproductive success, and the ability to modulate selfing would be a powerful tool in increasing yield.

Materials and methods

Plant materials and growth conditions

All *A. thaliana* seeds (Col-0, C24, transgenic lines, T-DNA insertion mutants and CRISPR/Cas9 deletion mutants) were sterilized and cold stratified at 4°C for 3 days. Seedlings were germinated on half Murashige and Skoog (1/2 MS) medium plates supplemented with 0.4% (w/v) phytoagar (pH 5.8) and 1% (w/v) sucrose. Seedlings were grown at 22°C under 16-h light for 7 days, and then transferred to Sunshine #1 soil supplemented with Plant Prod All Purpose Fertilizer 20-20-20 (1 g/L water). All plants were grown in chambers under a 16-h light/8-h dark growth cycle at 22°C, with humidity kept under 50%.

For the Col-0 accession experiments, the *Ah-SCR13 Ah-SRK13 Ah-ARC1* #2 Col-0 line (Zhang et al., 2019) was crossed to the *atg7-2* mutant (Col-0 accession; Chung et al., 2010) and *atg5-1* mutant (Thompson et al., 2005). For the C24 accession experiments, the *SI-C24 #15-1* line (with *AlSCRb AlSRKb*; Iwano et al., 2015) was crossed to the *atg7-9* mutant (C24 accession; see below). All transgenic lines were genotyped using primers found in Supplemental Table S1. For the C24 accession, plants were genotyped for $AlSCR_b$, $AlSRK_b$, and *atg7-9*. Progeny was analyzed in the F_2 generation for all three crosses. For SI-Col-0 *GFP-ATG8a*, the *Ah-SCR13 Ah-SRK13 Ah-ARC1 #2* Col-0 line (Zhang et al., 2019), was crossed into the *ProUBQ10:GFP-ATG8a* line (Col-0 accession; Kim et al., 2013), and the resulting F_1 progeny was used for all imaging.

Plasmid construction and plant transformation

The *atg7-9* CRISPR/Cas9 deletion mutation was generated in C24 using previously described methods in the Col-0 accession (Doucet et al., 2019a, 2019b). The final pBEE401E vector contained two guide RNAs targeting exons 3 and 8 of *ATG7* (Supplemental Figure S1). *A. thaliana* C24 plants were transformed using floral dip (Clough and Bent, 1998), and plants were dipped twice, 3 days apart, to maximize transformation efficiency. T1 seeds were collected and germinated on soil, and 1-week-old seedlings were sprayed with BASTA herbicide to select for transformants. PCR was used to confirm transformants (BASTA marker) and the presence of *atg7* mutations (deletions of the exons 3–8 region; Supplemental Figure S1). These *atg7* deletion mutants were then verified through sequencing of regions flanking the deletions. The *atg7* mutants showed a wild-type plant and flower morphology, along with the accelerated senescence typically seen in *atg* mutants (Thompson et al., 2005; Avila-Ospina et al., 2014). One homozygous mutant, *atg7-9*, from the T2 generation was crossed to the *SI-C24 #15-1* line, and all data were collected in the F_2 generation of this cross (F_4 generation for *atg7-9*).

Confocal microscopy

A. thaliana SI-Col-0 plants carrying the *ProUBQ10:GFP-ATG8a* construct were manually pollinated using pollen from the SI-Col-0 line or wild-type Col-0. Pistils were

removed at 10-min postpollination and images of autophagosomes were taken at 15-min postpollination. All images were captured using a Leica TCS SP8 confocal microscope using a 40× oil-immersion objective. Imaging was completed using a 488-nm laser at 35% intensity, captured using either a HyD detector for GFP (495–545-nm emission, 100% gain, 2.0 AU pinhole diameter) or a photomultiplier tube detector for bright field (700–850 V). Leica LAS AF lite in combination with ImageJ was used for image processing and puncta counting. GFP punctae were counted in stigmatic papillae cell areas directly adjacent to SI-Col-0 pollen or Col-0 pollen, and an equivalent cell area in unpollinated samples.

Assays for pollen hydration, aniline blue staining, and seed set

All postpollination assays used manual pollinations and were conducted as described in Lee et al. (2020). For the SI-C24 plants, late stage 12 pistils were first emasculated and wrapped in plastic wrap overnight prior to pollination. For the SI-Col-0 plants, the pistils did not require emasculation due to the approach herkogamy phenotype (Zhang et al. 2019), and freshly opened flowers with unpollinated pistils were selected for these assays. All pollinations were completed at humidity levels under 50% for consistency. Pollen hydration assays were conducted by removing and mounting pistils on 1/2 MS, and lightly pollinating the stigmatic surface using a single anther. Images were taken at 0- and 10-min postpollination using a Nikon sMz800 microscope, and pollen grains on the stigmatic surface were randomly selected for measurements using the NIS-elements imaging software. For the aniline blue staining, one anther was used to lightly pollinate each pistil, and the pistils were then collected at 2- and 24-h postpollination for staining as described in Lee et al. (2020). The aniline blue-stained pistils were mounted on a slide with sterile water, flattened with the coverslip, and imaged at 10× magnification on a Zeiss Axioscope2 Plus fluorescent microscope. Aniline blue images were captured using the UV laser (150 ms exposure, 2 gain), and bright-field images were captured using the built-in halogen lamp (20 ms exposure, 2 gain). For seed counts, pistils were manually pollinated with a single anther and were left for 10–14 days. The maturing siliques were then removed and cleared in 70% (v/v) ethanol for 3–5 days, or until seeds were visible (Beuder et al., 2020). Siliques were then mounted on a dry slide with the septum facing upwards and imaged using a Nikon sMz800 microscope, and seeds were counted using the NIS-elements imaging software.

Statistical analyses

One-way analysis of variance (ANOVA) with Tukey's honest significant difference (HSD) post-hoc tests were performed using SPSS (IBM, Armonk, NY, USAs), and Student's *t* tests were performed using Excel (Microsoft Redmond, WA, USA).

Accession numbers

Gene identifiers for the autophagy genes are as follows: ATG5, At5g17290, and ATG7 At5g45900.

Supplemental data

The following materials are available in the online version of this article.

Supplemental Figure S1. Generation of the *ATG7* CRISPR/Cas9 deletion mutation in the C24 accession.

Supplemental Figure S2. Representative images of flowering plants for the SI-C24 and *atg7-9* mutant plants in the C24 accession.

Supplemental Figure S3. Representative images of aniline blue-stained pistils at 2 h following pollination with SI-Col-0 or Col-0 pollen.

Supplemental Figure S4. Representative images of aniline blue-stained pistils at 2 h following pollination with SI-C24 or C24 pollen.

Supplemental Figure S5. Representative images of cleared siliques used in seed counting for control and SI plants with the *atg7* mutation.

Supplemental Table S1. Primer sequences.

Acknowledgments

We thank Laura Canales and Arjun Sharma for technical assistance, and members of the Goring lab for critically reading this article. We are very grateful to Seiji Takayama (Nara Institute of Science and Technology; University of Tokyo) for providing the *SI-C24 #15-1* seeds (*A. thaliana* C24), Richard Vierstra (Washington University in St Louis), and Peter Bozhkov (Swedish University of Agricultural Sciences) for providing *atg7-2* and *atg5-1* mutant seeds (*A. thaliana* Col-0), and Marisa Otegui (University of Wisconsin-Madison) for providing the *ProUBQ10:GFP-ATG8a* seeds (*A. thaliana* Col-0).

Funding

This research was supported by a grant from Natural Sciences and Engineering Research Council of Canada to D.R.G., S.R.M. was supported by the Rustom H. Dastur Graduate Scholarship, and H.K.L. was supported by an Ontario Graduate Scholarship.

Conflict of interest statement. None declared.

References

Abhinandan K, Sankaranarayanan S, Macgregor S, Goring DR, Samuel MA (2021) Cell-cell signaling during the Brassicaceae self-incompatibility response. Trends Plant Sci S1360-1385(21)00303-4, https://doi.org/10.1016/j.tplants.2021.10.011

Adhikari PB, Liu X, Wu X, Zhu S, Kasahara RD (2020) Fertilization in flowering plants: an odyssey of sperm cell delivery. Plant Mol Biol **103**: 9–32

Avila-Ospina L, Moison M, Yoshimoto K, Masclaux-Daubresse C (2014) Autophagy, plant senescence, and nutrient recycling. J Exp Bot **65:** 3799–3811

Beuder S, Dorchak A, Bhide A, Moeller SR, Petersen BL, MacAlister CA (2020) Exocyst mutants suppress pollen tube growth and cell wall structural defects of hydroxyproline O-arabinosyltransferase mutants. Plant J **103:** 1399–1419

Boggs NA, Nasrallah JB, Nasrallah ME (2009) Independent S-locus mutations caused self-fertility in *Arabidopsis thaliana*. Plos Genet **5**: e1000426

Brillada C, Teh OK, Ditengou FA, Lee CW, Klecker T, Saeed B, Furlan G, Zietz M, Hause G, Eschen-Lippold L, et al. (2021) Exocyst subunit Exo70B2 is linked to immune signaling and autophagy. Plant Cell **33:** 404–419

Chung T, Phillips AR, Vierstra RD (2010) ATG8 lipidation and ATG8-mediated autophagy in Arabidopsis require ATG12 expressed from the differentially controlled ATG12A AND ATG12B loci. Plant J **62:** 483–493

Clough SJ, Bent AF (1998) Floral dip: a simplified method for Agrobacterium-mediated transformation of *Arabidopsis thaliana*. Plant J **16:** 735–743

Dickinson H (1995) Dry stigmas, water and self-incompatibility in Brassica. Sex Plant Reprod **8**: 1–10

Ding X, Zhang X, Otegui MS (2018) Plant autophagy: new flavors on the menu. Curr Opin Plant Biol **46:** 113–121

Doucet J, Lee HK, Udugama N, Xu J, Qi B, Goring DR (2019a) Investigations into a putative role for the novel BRASSIKIN pseudokinases in compatible pollen-stigma interactions in *Arabidopsis thaliana*. BMC Plant Biol **19:** 549

Doucet J, Truong C, Frank-Webb E, Lee HK, Daneva A, Gao Z, Nowack MK, Goring DR (2019b) Identification of a role for an E6-like 1 gene in early pollen-stigma interactions in *Arabidopsis thaliana*. Plant Reprod **32:** 307–322

Durand E, Chantreau M, Le Veve A, Stetsenko R, Dubin M, Genete M, Llaurens V, Poux C, Roux C, Billiard S, et al. (2020) Evolution of self-incompatibility in the Brassicaceae: lessons from a textbook example of natural selection. Evol Appl **13**: 1279–1297

Elleman C, Dickinson H (1996) Identification of pollen of components regulating the responses in stigmatic Brassica oleracea. New Phytol **133**: 197–205

Fujii S, Shimosato-Asano H, Kakita M, Kitanishi T, Iwano M, Takayama S (2020) Parallel evolution of dominant pistil-side self-incompatibility suppressors in Arabidopsis. Nat Commun **11:** 1404

Goring DR (2017) Exocyst, exosomes, and autophagy in the regulation of Brassicaceae pollen-stigma interactions. J Exp Bot **69**: 69–78

Goubet PM, Berges H, Bellec A, Prat E, Helmstetter N, Mangenot S, Gallina S, Holl AC, Fobis-Loisy I, Vekemans X, et al. (2012) Contrasted patterns of molecular evolution in dominant and recessive self-incompatibility haplotypes in Arabidopsis. PLoS Genet **8:** e1002495

Gu T, Mazzurco M, Sulaman W, Matias DD, Goring DR (1998) Binding of an arm repeat protein to the kinase domain of the S-locus receptor kinase. Proc Natl Acad Sci USA **95:** 382–387

Guo YL, Zhao X, Lanz C, Weigel D (2011) Evolution of the S-locus region in Arabidopsis relatives. Plant Physiol **157**: 937–946

Indriolo E, Goring DR (2014) A conserved role for the ARC1 E3 ligase in Brassicaceae self-incompatibility. Front Plant Sci **5:** 181

Indriolo E, Goring DR (2016) Yeast two-hybrid interactions between *Arabidopsis lyrata* S Receptor Kinase and the ARC1 E3 ligase. Plant Signal Behav **11:** e1188233

Indriolo E, Safavian D, Goring DR (2014a) The ARC1 E3 ligase promotes two different self-pollen avoidance traits in Arabidopsis. Plant Cell **26**: 1525–1543

Indriolo E, Safavian D, Goring DR (2014b) Signaling events in pollen acceptance or rejection in the Arabidopsis species. Sexual Reproduction in Animals and Plants, Springer, Berlin/Heidelberg, Germany, pp 255–271

Indriolo E, Tharmapalan P, Wright SI, Goring DR (2012) The ARC1 E3 ligase gene is frequently deleted in self-compatible Brassicaceae species and has a conserved role in *Arabidopsis lyrata* self-pollen rejection. Plant Cell **24:** 4607–4620

Iwano M, Ito K, Fujii S, Kakita M, Asano-Shimosato H, Igarashi M, Kaothien-Nakayama P, Entani T, Kanatani A, Takehisa M, et al. (2015) Calcium signalling mediates self-incompatibility response in the Brassicaceae. Nat Plants **1**: 15128

Jamshed M, Sankaranarayanan S, Abhinandan K, Samuel MA (2020) Stigma receptivity is controlled by functionally redundant MAPK pathway components in Arabidopsis. Mol Plant **13**: 1582–1593

Jany E, Nelles H, Goring DR (2019) The molecular and cellular regulation of Brassicaceae self-incompatibility and self-pollen rejection. Int Rev Cell Mol Biol **343**: 1–35

Johnson MA, Harper JF, Palanivelu R (2019) A fruitful journey: pollen tube navigation from germination to fertilization. Annu Rev Plant Biol **70:** 809–837

Kenney P, Sankaranarayanan S, Balogh M, Indriolo E (2020) Expression of *Brassica napus* GLO1 is sufficient to breakdown artificial self-incompatibility in *Arabidopsis thaliana*. Plant Reprod **33:** 159–171

Kim J, Lee H, Lee HN, Kim SH, Shin KD, Chung T (2013) Autophagy-related proteins are required for degradation of peroxisomes in Arabidopsis hypocotyls during seedling growth. Plant Cell **25**: 4956–4966

Kusaba M, Dwyer K, Hendershot J, Vrebalov J, Nasrallah JB, Nasrallah ME (2001) Self-incompatibility in the genus Arabidopsis: characterization of the S locus in the outcrossing A. Lyrata and its autogamous relative A. thaliana. Plant Cell **13**: 627–644

Lee HK, Macgregor S, Goring DR (2020) A toolkit for teasing apart the early stages of pollen-stigma interactions in *Arabidopsis thaliana*. Methods Mol Biol **2160**: 13–28

Lin Y, Zeng Y, Zhu Y, Shen J, Ye H, Jiang L (2021) Plant Rho GTPase signaling promotes autophagy. Mol Plant **14:** 905–920

Mizuta Y, Higashiyama T (2018) Chemical signaling for pollen tube guidance at a glance. J Cell Sci **131**: jcs208447

Nasrallah JB (2019) Self-incompatibility in the Brassicaceae: regulation and mechanism of self-recognition. Curr Top Dev Biol **131**: 435–452

Nasrallah ME, Liu P, Sherman-Broyles S, Boggs NA, Nasrallah JB (2004) Natural variation in expression of self-incompatibility in *Arabidopsis thaliana*: implications for the evolution of selfing. Proc Natl Acad Sci USA **101:** 16070–16074

Palanivelu R, Tsukamoto T (2012) Pathfinding in angiosperm reproduction: pollen tube guidance by pistils ensures successful double fertilization. Wiley Interdisciplin Rev Dev Biol **1:** 96–113

Rozier F, Riglet L, Kodera C, Bayle V, Durand E, Schnabel J, Gaude T, Fobis-Loisy I (2020) Live-cell imaging of early events following pollen perception in self-incompatible *Arabidopsis thaliana*. J Exp Bot **71:** 2513–2526

Safavian D, Goring DR (2013) Secretory activity is rapidly induced in stigmatic papillae by compatible pollen, but inhibited for self-incompatible pollen in the Brassicaceae. PLoS One **8**: e84286

Safavian D, Jamshed M, Sankaranarayanan S, Indriolo E, Samuel MA, Goring DR (2014) High humidity partially rescues the *Arabidopsis thaliana* exo70A1 stigmatic defect for accepting compatible pollen. Plant Reprod **27**: 121–127

Safavian D, Zayed Y, Indriolo E, Chapman L, Ahmed A, Goring DR (2015) RNA silencing of exocyst genes in the stigma impairs the acceptance of compatible pollen in Arabidopsis. Plant Physiol **169:** 2526–2538

Samuel MA, Chong YT, Haasen KE, Aldea-Brydges MG, Stone SL, Goring DR (2009) Cellular pathways regulating responses to compatible and self-incompatible pollen in Brassica and Arabidopsis stigmas intersect at Exo70A1, a putative component of the exocyst complex. Plant Cell **21:** 2655–2671

Sankaranarayanan S, Jamshed M, Samuel MA (2015) Degradation of glyoxalase I in *Brassica napus* stigma leads to self-incompatibility response. Nat Plants **1**: 15185

Scandola S, Samuel MA (2019) A Flower-Specific Phospholipase D Is a Stigmatic Compatibility Factor Targeted by the Self-Incompatibility Response in *Brassica napus*. Curr Biol **29:** 506–512 e504

Schierup MH, Mable BK, Awadalla P, Charlesworth D (2001) Identification and characterization of a polymorphic receptor kinase gene linked to the self-incompatibility locus of *Arabidopsis lyrata*. Genetics **158:** 387–399

Shimizu KK, Shimizu-Inatsugi R, Tsuchimatsu T, Purugganan MD (2008) Independent origins of self-compatibility in *Arabidopsis thaliana*. Mol Ecol **17:** 704–714

Shimizu KK, Tsuchimatsu T (2015) Evolution of selfing: recurrent patterns in molecular adaptation. Ann Rev Ecol Evol Syst **46:** 593–622

Stone SL, Anderson EM, Mullen RT, Goring DR (2003) ARC1 is an E3 ubiquitin ligase and promotes the ubiquitination of proteins during the rejection of self-incompatible Brassica pollen. Plant Cell **15:** 885–898

Stone SL, Arnoldo M, Goring DR (1999) A breakdown of Brassica self-incompatibility in ARC1 antisense transgenic plants. Science **286:** 1729–1731

Thompson AR, Doelling JH, Suttangkakul A, Vierstra RD (2005) Autophagic nutrient recycling in Arabidopsis directed by the ATG8 and ATG12 conjugation pathways. Plant Physiol **138**: 2097–2110

Tsuchimatsu T, Goubet PM, Gallina S, Holl AC, Fobis-Loisy I, Berges H, Marande W, Prat E, Meng D, Long Q, et al. (2017) Patterns of polymorphism at the self-incompatibility locus in 1,083 *Arabidopsis thaliana* genomes. Mol Biol Evol **34:** 1878–1889

Tsuchimatsu T, Suwabe K, Shimizu-Inatsugi R, Isokawa S, Pavlidis P, Stadler T, Suzuki G, Takayama S, Watanabe M, Shimizu KK (2010) Evolution of self-compatibility in Arabidopsis by a mutation in the male specificity gene. Nature **464**: 1342–1346

Young PG, Passalacqua MJ, Chappell K, Llinas RJ, Bartel B (2019) A facile forward-genetic screen for Arabidopsis autophagy mutants reveals twenty-one loss-of-function mutations disrupting six ATG genes. Autophagy **15:** 941–959

Zhang T, Zhou G, Goring DR, Liang X, Macgregor S, Dai C, Wen J, Yi B, Shen J, Tu J, Fu T, Ma C (2019) Generation of transgenic self-incompatible *Arabidopsis thaliana* shows a genus-specific preference for self-incompatibility genes. Plants **8:** 570